

Influences of Climate Change on the Uptake and Storage of Anthropogenic CO₂ in the Global Ocean

LI Yangchun¹ (李阳春), XU Yongfu^{1*} (徐永福), CHU Min² (储敏), and YU Yongqiang³ (俞永强)

¹ State Key Laboratory of Atmospheric Boundary Layer Physics and Atmospheric Chemistry, Institute of Atmospheric Physics, Chinese Academy of Sciences, Beijing 100029

² National Climate Center, Beijing 100081

³ State Key Laboratory of Numerical Modeling for Atmospheric Sciences and Geophysical Fluid Dynamics, Institute of Atmospheric Physics, Chinese Academy of Sciences, Beijing 100029

(Received May 3, 2011; in final form October 3, 2011)

ABSTRACT

A global ocean general circulation model, called LASG/IAP Climate system ocean model (LICOM), is employed to study the influence of climate change on the uptake and storage of anthropogenic CO₂ in the global ocean. Two simulations were made: the control run (RUN1) with the climatological daily mean forcing data, and the climate change run (RUN2) with the interannually varying daily mean forcing data from the NCEP (National Centers for Environmental Prediction) of the US. The results show that the simulated distributions and storages of anthropogenic dissolved inorganic carbon (anDIC) from both runs are consistent with the data-based results. Compared with the data-based results, the simulations generate higher anDIC concentrations in the upper layer and lower storage amount of anDIC between the subsurface and 1000-m depth, especially in RUN1. A comparison of the two runs shows that the interannually varying forcing can enhance the transport of main water masses, so the rate of interior transport of anDIC is increased. The higher transfer rate of anDIC in RUN2 decreases its high concentration in the upper layer and increases its storage amount below the subsurface, which leads to closer distributions of anDIC in RUN2 to the data-based results than in RUN1. The higher transfer rate in RUN2 also induces larger exchange flux than in RUN1. It is estimated that the global oceanic anthropogenic CO₂ uptake was 1.83 and 2.16 Pg C yr⁻¹ in the two runs in 1995, respectively, and as of 1994, the global ocean contained 99 Pg C in RUN1 and 107 Pg C in RUN2 of anDIC, indicating that the model under the interannually varying forcing could take up 8.1% more anthropogenic carbon than the model under the climatological forcing. These values are within the range of other estimates based on observation and model simulation, while the estimates in RUN1 are near the low bound of other works. It is estimated that the variability of root mean square of the global air-sea anthropogenic carbon flux from the simulated monthly mean results of RUN2 with its seasonal cycle and long-term trend removed is 0.1 Pg C yr⁻¹. The most distinct anomalies appear to be in the tropical Pacific Ocean and the Southern Ocean.

Key words: anthropogenic CO₂, climate change, oceanic uptake, flux, variability

Citation: Li Yangchun, Xu Yongfu, Chu Min, et al., 2012: Influences of climate change on the uptake and storage of anthropogenic CO₂ in the global ocean. *Acta Meteor. Sinica*, **26**(3), 304–317, doi: 10.1007/s13351-012-0304-z.

1. Introduction

Since preindustrial times, a great amount of carbon dioxide (CO₂) has been released into the atmosphere due to human activities, about half of which has remained in the atmosphere and the rest has been taken up by the ocean and land, so the content of at-

mospheric CO₂ has increased by over 100 ppmv. The CO₂ emitted by human resources is man-made CO₂, often called anthropogenic CO₂. Sundquist (1993) pointed out that anthropogenic CO₂ is a biogeochemical perturbation of truly geologic proportions. It has been estimated that the oceans have absorbed over 40% of anthropogenic CO₂ from the fossil fuel comb-

Supported by the National Basic Research and Development (973) Program of China (2010CB951802), China Meteorological Administration Special Public Welfare Research Fund (GYHY2008416022), and National Natural Science Foundation of China (40730106).

*Corresponding author: xyf@mail.iap.ac.cn.

©The Chinese Meteorological Society and Springer-Verlag Berlin Heidelberg 2012

ustion and cement production (Sabine et al., 2004; Solomon et al., 2007). However, the precise estimate of distributions and storage of anthropogenic CO₂ in the ocean is still controversial.

Although anthropogenic CO₂ cannot be directly measured, it can be estimated through certain approaches. Basically, there are two categories of approaches for estimating the inventory and uptake of anthropogenic CO₂: the data-based and model-based estimates. Using the measurements of partial pressure of CO₂ (pCO₂) in the surface water and air, the air-sea CO₂ exchange flux can be calculated, from which the uptake of anthropogenic CO₂ can be derived if the exchange flux of natural CO₂ is known. A typical estimate can be found in Takahashi et al. (2002), who obtained a CO₂ exchange flux of 1.54 Pg C yr⁻¹ in 1995.

Using the observed dissolved inorganic carbon (DIC), anthropogenic CO₂ can be derived from the DIC concentration difference between current and preindustrial conditions, which is often called the ΔC^* method (Gruber et al., 1996). Another approach using the observed DIC is called multiple linear regression analysis, which is used to estimate the temporal change of anthropogenic CO₂ (Levine et al., 2008). Using the DIC and DI14C (dissolved inorganic radiocarbon) data as well as results of OGCMs (ocean general circulation models), Sweeney et al. (2007) obtained the 1995 CO₂ flux of 1.3±0.5 Pg C yr⁻¹, which is less than the estimate of 1.7±0.4 Pg C yr⁻¹ by Gruber et al. (2009) using the inversion method of Gloor et al. (2003) based on observed DIC data. Recently, Khatiwala and Hall (2009) used a new inversion method to reconstruct the history of anthropogenic CO₂ concentrations in the global ocean exclusive of the Arctic Ocean. They obtained the inventory estimate of 114±22 Pg C for the year 1994, which is close to the estimate of 106±21 Pg C in the ocean south of 65°N by the ΔC^* method (Sabine et al., 2004).

In addition to the estimations based on the marine observations, there are estimations based on the atmospheric observations, including the inversion of atmospheric O₂/N₂ (Bender et al., 2005; Manning and Keeling, 2006) and atmospheric CO₂ concentrations (Gurney et al., 2004). Using the air-sea disequilib-

rium of CO₂ isotopic (DIC $\delta^{13}C$), Gruber and Keeling (2001) obtained an annual oceanic anthropogenic CO₂ uptake of 1.5±0.9 Pg C, which is 0.5 Pg C smaller than the estimate of 2.0 Pg C by Joos et al. (1999) using atmospheric $\delta^{13}C$ and CO₂ data of the same period 1985–1995.

The other category of approaches for estimating anthropogenic CO₂ is to directly use the ocean carbon-cycle model. Maier-Reimer and Hasselmann (1987) first employed an OGCM to study the inorganic carbon cycle. The improvement to the carbon-cycle model is related to the inclusion of biological processes (Bacastow and Maier-Reimer, 1990; Six and Maier-Reimer, 1996). Many studies using the three-dimensional ocean carbon-cycle models have been carried out. Sarmiento et al. (1992) proposed a special model of anthropogenic CO₂ with the perturbation method, which provides a direct simulation of the uptake and storage of anthropogenic CO₂. The simulated results are quite useful for the comparison of OGCMs. The first phase of the Ocean Carbon Model Intercomparison Project (OCMIP) indicates that the simulated uptake of anthropogenic CO₂ from the four OGCMs deviates within ±19% (Orr et al., 2001). In the comparison of 13 OGCMs participating in the second phase of OCMIP, Doney et al. (2004) found that a large difference substantial in biogeochemical fields among the models is caused by the errors in model physics. It is seen that different physical parameterization schemes and numerical procedures are one of the main causes for the large differences of simulated results between the models (Solomon et al., 2007).

Currently, many researchers are paying more attention to interannual variability of the oceanic uptake of atmospheric CO₂ using primitive equation OGCM with biogeochemical processes (Le Quéré et al., 2000; Obata and Kitamura, 2003; McKinley et al., 2004; Wetzel et al., 2005; Wang et al., 2006; Rodgers et al., 2008). However, reports have not been seen about the direct simulation of the influence of climate change on the uptake of anthropogenic CO₂.

Many Chinese scientists have been working on the scientific issues of ocean carbon cycle, and have developed different models in one to three dimensions. Dong et al. (1994) and Pu and Wang (2001) con-

ducted offline runs of two-dimensional carbon cycle models with biological processes in the Atlantic and Indian oceans, respectively. The physical fields were obtained from the Institute of Atmospheric Physics (IAP) OGCM with four vertical levels. Xing (2000) studied the influence of biological processes on the carbon cycle in a global OGCM. Using MOM2 (Modular Ocean Model version 2), Jin and Shi (2001) investigated the uptake and storage of anthropogenic CO₂ in the global carbon-cycle model with biological processes. Xu and Li (2009) estimated the storage of anthropogenic carbon in the IAP global OGCM named L30T63, and found that although the simulated result of inventories is within the range estimated by other researchers, it is smaller than the data-based estimate. In their study, climatological monthly mean forcing was used to drive the OGCM.

The objective of this work is to use a new generation OGCM developed by IAP to estimate the uptake and storage of anthropogenic CO₂ in the world ocean with two sets of different forcing data, the climatological daily mean forcing, and the interannually varying daily mean forcing. The perturbation method is employed to study how climate change affects the uptake and storage of anthropogenic CO₂ in different regions, and to explore the temporal variation in the response of anthropogenic CO₂ to climate change. In the following text, the observed data of anthropogenic carbon were provided by the Global Ocean Data Analysis Project (GLODAP) (Key et al., 2004) and obtained from the Carbon Dioxide Information Analysis Center (CDIAC, <http://cdiac.ornl.gov>). The data were mainly collected between 1985 and 1999. Some data from the Geochemical Ocean Sections Program (GEOSECS) carried out during the 1970s were also included.

2. Model description

2.1 Ocean general circulation model

The global OGCM named LICOM (LASG/IAP Climate system Ocean Model; LASG/IAP stands for State Key Laboratory of Numerical Modeling for Atmospheric Sciences and Geophysical Fluid Dynamics/Institute of Atmospheric Physics) is adopted in

this work. A detailed description of the model can be found in Liu et al. (2004). The model domain is 78°S–90°N, 0°–360°E with a horizontal resolution of 2°×2°. There are 30 vertical levels, among which the upper 15 levels are equally spaced and the other 15 levels are unequally spaced. The top level is 10 m in depth, and the maximum depth is 5600 m.

The main features of the model include the free surface, η -vertical coordinates, the Arakawa B-grid scheme, the penetration of solar radiation, the Richardson number-dependent turbulent mixing process in the tropical ocean, the isopycnal mixing scheme (often called GM90) with an eddy-induced transport velocity by Gent and McWilliams (1990) and Gent et al. (1995), etc. Both isopycnal and thickness (skew) diffusivities in GM90 are taken to be $1.0 \times 10^3 \text{ m}^2 \text{ s}^{-1}$. The vertical diffusion coefficient is set to be a constant of $0.3 \times 10^4 \text{ m}^2 \text{ s}^{-1}$. It is estimated from the observations that these diffusion coefficients have a large range (McWilliams et al., 1983; Danabasoglu and McWilliams, 1995). In the current OGCMs, the GM90 diffusivities are generally set to $10^3 \text{ m}^2 \text{ s}^{-1}$, and the vertical diffusivity is set to 0.3 (or 0.5) $\times 10^{-4} \text{ m}^2 \text{ s}^{-1}$ (Danabasoglu and McWilliams, 1995; England and Hirst, 1997; Duffy et al., 1997).

The OGCM is driven at the surface by climatological daily mean boundary conditions of thermal fluxes, sea surface temperature (SST), and wind stress, which are 62-yr mean over the period 1948–2009 from the NCEP/NCAR reanalysis project. The climatological monthly mean sea-surface salinity (SSS) from WOA98 (<http://www.nodc.noaa.gov/>) is adopted because of the absence of the daily mean data. All simulations presented here were initialized from the observed annual mean climatological temperature and salinity of the Levitus data (Levitus and Boyer, 1994; Levitus et al., 1994). The model was integrated for over 2000 years. For the simulation of oceanic anthropogenic carbon uptake, we restarted the model from the above equilibrated ocean circulation of the OGCM, and included an additional passive tracer for anthropogenic CO₂.

2.2 Anthropogenic CO₂ model

The equation proposed by Sarmiento et al. (1992)

is used to relate partial pressure of anthropogenic CO₂ to anthropogenic dissolved inorganic carbon (anDIC) in the ocean. Based on this perturbation method, we solve the advection-diffusion equation of anthropogenic CO₂ in the ocean. The ocean surface layer exchanges anthropogenic CO₂ with the atmosphere, while the atmosphere is treated as a well-mixed box. The flux of air-sea anthropogenic carbon can be written as:

$$\text{Flux} = S_g(1 - \gamma_{\text{ice}})(\delta p\text{CO}_{2\text{a}} - \delta p\text{CO}_{2\text{o}}), \quad (1)$$

where γ_{ice} is the fraction of sea ice cover, $\delta p\text{CO}_{2\text{a}}$ and $\delta p\text{CO}_{2\text{o}}$ indicate the perturbations of the partial pressure of CO₂ in the atmosphere and the ocean, relative to their preindustrial values. Here, the year of 1800 is defined as the beginning of industrial revolution. The concentration of anthropogenic carbon in both the ocean and atmosphere is defined as zero at the beginning of the simulation (time 0), which is considered as the year 1800.

The exchange coefficient (S_g) of CO₂ at the air-sea interface is the product of transfer velocity and solubility of CO₂. The transfer velocity from Wanninkhof's (1992) equation is a function of wind speed and sea water temperature. The daily mean data of wind speed are also from NCEP. The time history of atmospheric $p\text{CO}_2$ is prescribed by using the values at the beginning and middle of each year, which is taken from Enting et al. (1994), with some supplement from the recently observed data from CDIAC (<http://cdiac.ornl.gov>). Then, the atmospheric CO₂ values are linearly interpolated into each time step.

2.3 Numerical experiment design

After 2000-yr integration of LICOM, the anthropogenic carbon model was incorporated into this OGCM. Two numerical experiments were conducted: a control run (RUN1) and a climate change run (RUN2). RUN1 was integrated for a total of 210 yr from 1800 to 2009 under the forcing of the same climatological daily mean data and the above prescribed atmospheric $p\text{CO}_2$ data. RUN2 was initiated from the results of RUN1 at the end of 1947 and integrated for 62 yr from 1948 to 2009 under the forcing of interannually varying daily mean forcing data and the same

time series of atmospheric CO₂. The wind speed for the calculation of the air-sea anthropogenic CO₂ flux used in both runs is from NCEP. RUN1 uses the climatological daily mean wind speed while RUN2 uses the interannually varying daily mean wind speed.

3. Results and discussion

3.1 Distributions of anthropogenic CO₂ under different forcings

The simulated and data-based anDIC concentrations at 50 m in the 1990s are shown in Fig. 1. If not stated otherwise, in the following text, all simulated results are the 1990s average in order to correspond to the observation data period. The concentration of anDIC at 50 m is attributed to the strength of local uptake and ocean interior transport. The data-based results show that low anDIC concentrations occur in the equatorial and high-latitude regions, especially in the equatorial Pacific and the Southern Ocean. The upwelling in the equatorial region, especially the equatorial Pacific Ocean, leads to the low anDIC concentration because the anthropogenic CO₂-poor deep water is brought up to the surface. The strong vertical exchange of water mass in the Southern Ocean transports the absorbed anthropogenic CO₂ into the deep water quickly, so the upper water contains low concentrations of anDIC. With the weak vertical movement and diffusion, the subtropical region has high concentrations of anDIC after its long contact with the atmosphere and the transport by the wind-driven circulations from both the north and south. The simulated distribution characteristics are in good agreement with the data-based results from WOCE (World Ocean Circulation Experiment), although the simulated values are larger than the data-based estimates because of the weak mixing process in the upper ocean. The difference (Fig. 1c) between the two runs shows that the overestimate of anDIC concentrations in RUN1 is reduced in RUN2 with the interannually varying forcing, with the largest difference over 6 $\mu\text{mol kg}^{-1}$ in the eastern equatorial Pacific Ocean.

The column inventory of anDIC is shown in Fig. 2. Because of the formation of ocean water mass and interior transport, the main storage areas of passive

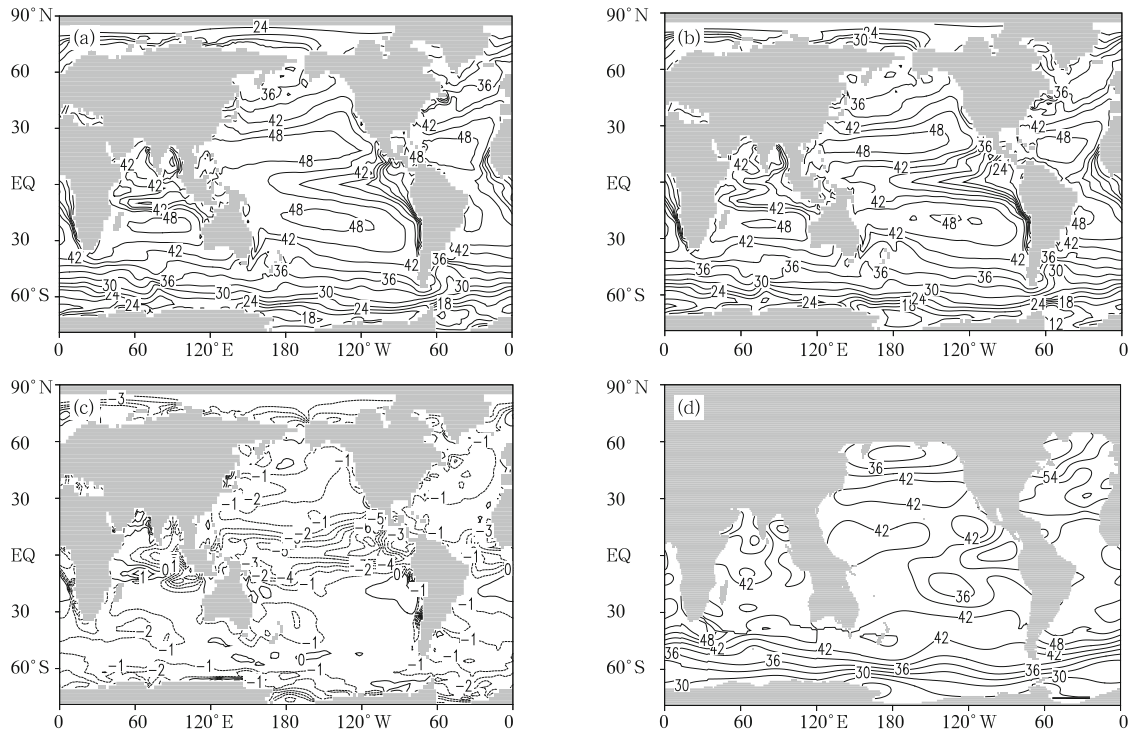


Fig. 1. Distributions of anthropogenic carbon concentrations ($\mu\text{mol kg}^{-1}$) at 50 m in the 1990s. (a) RUN1, (b) RUN2, (c) difference between RUN1 and RUN2 (RUN2–RUN1), and (d) data-based results. Contour intervals are 3 $\mu\text{mol kg}^{-1}$ in (a, b, d), and 1 $\mu\text{mol kg}^{-1}$ in (c).

tracers are located in the subtropical regions of different ocean basins, while due to the formation of the North Atlantic Deep Water (NADW), the western North Atlantic is the area with the largest anDIC column inventory of over 80 mol m^{-2} . The simulated results are basically consistent with the data-based estimates on these features. The main difference is that in the western equatorial Pacific, the data-based estimates show the minimum values that are probably caused by the shallow isopycnal surfaces (Key et al., 2004). However, like other models (Orr et al., 2001), the LICOM model does not give this feature yet. Compared with GFDL, Hadley, and MPIM models, in which strong vertical movement generates unrealistic column inventory of over 60 mol m^{-2} in the Southern Ocean (Orr et al., 2001), our results are more reasonable.

The anDIC column inventory in RUN2 is distinctly larger than that in RUN1 in most regions (Fig. 2c), especially in Northwest Atlantic and the western tropical Pacific. The difference of the column inven-

tory between the two runs illustrates that the physical fields caused by the different physical forcings produce different uptake rates and transport strengths of anDIC in these regions. Because climatological means of the two forcing datasets are identical, the difference in ocean circulation must result from nonlinear processes such as advection, convection, etc. For example, the largest difference in anthropogenic carbon column inventory between the two runs occurs in Northwest Atlantic, where in RUN2 the mixed depth shows strong interannual and interdecadal variations, which are very significant during the climate events such as ENSO, AMO (Atlantic Multidecadal Oscillation), etc. However, there is little variability on the interannual and decadal timescales in mixed layer depth in RUN1. Thus, when the mixed layer is deep (figure omitted), more anthropogenic carbon is transported into the deep water quickly, leading to the enhancement of penetration depth of anthropogenic carbon.

Furthermore, according to the observations, Sabine et al. (2004) estimated that the global ocean

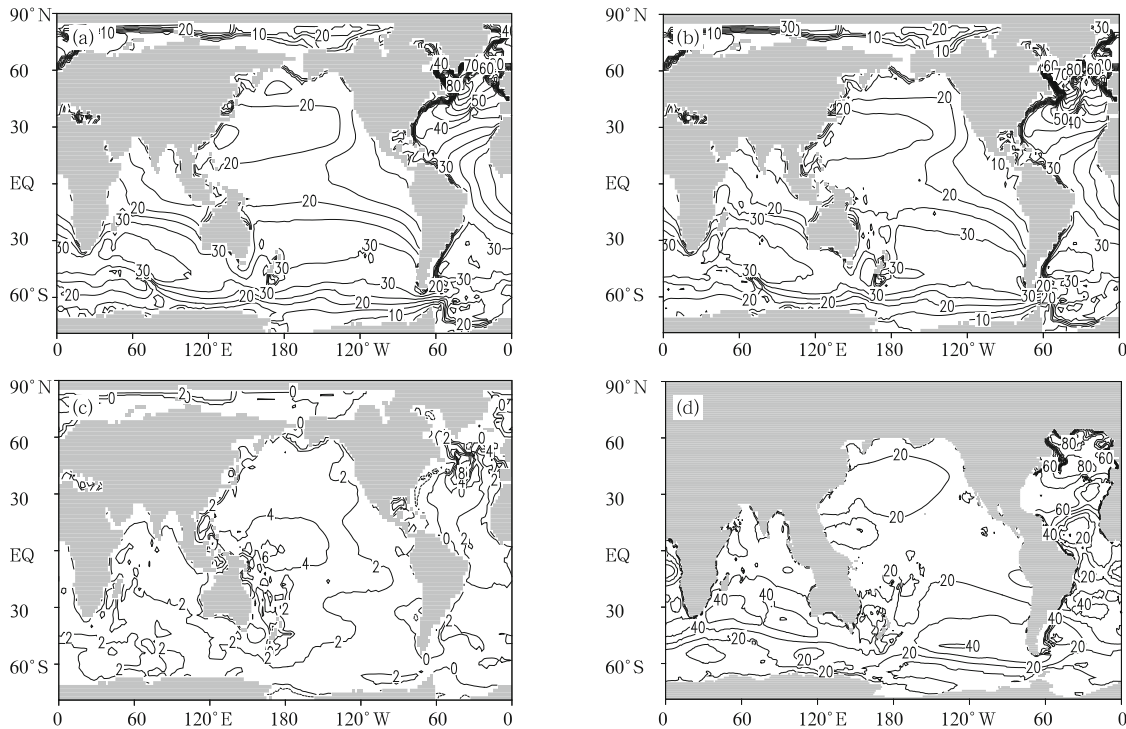


Fig. 2. Distributions of anthropogenic CO₂ column inventory (mol m^{-2}) in the 1990s. (a) RUN1, (b) RUN2, (c) difference between RUN1 and RUN2 (RUN2–RUN1), and (d) data-based results. Contour intervals are 5 mol m^{-2} in (a, b, d), and 2 mol m^{-2} in (c).

contained $118 \pm 19 \text{ Pg C}$ of anthropogenic carbon as of 1994. Waugh et al. (2006) used the observed CFC-12 data and simulated anthropogenic carbon results to obtain a global ocean storage of $94\text{--}121 \text{ Pg C}$ as of 1994. Our simulations estimate that the global ocean contained 99 (RUN1) and 107 Pg C (RUN2) anthropogenic carbon, which is within the range of the data-based estimates. It seems that the estimate from RUN1 is closer to the low bound of data-based estimates.

The lower concentration and larger column inventory in RUN2 indicate that the interior transport is stronger in RUN2 than in RUN1. As a result, the difference of the column inventory between the two runs in the tropical ocean is attributed to the deeper penetration depth of anDIC in RUN2. The zonal mean vertical distributions of anDIC in the Pacific and Indian Oceans are shown in Fig. 3. The smallest penetration occurs in the tropical ocean and the high latitudes in the data-based results and our simulations because of the shallow isopycnal surface. As a result,

vertical distributions of anDIC in the Pacific and Indian Oceans form the same “W” shape as other tracers such as temperature, CFC-11, etc. Compared with the data-based estimate, the carbon storage amount from the two runs between the subsurface and the 1000-m depth is not sufficient since the penetration depths of isolines are shallower than those of the data-based ones. Compared with RUN1, the penetration depth in RUN2 is deeper. For example, the largest penetration of the $5 \mu\text{mol kg}^{-1}$ contour in RUN2 is over 200 m deeper than that in RUN1 in both the Southern and Northern Hemispheres, even though for the shallowest penetration at 10°N the difference is near 250 m. It is known from the simulated zonally averaged isopycnals shown in Fig. 3 that the main storage region of anDIC is consistent with that of deep isopycnals. This is in agreement with the data-based results by Sabine et al. (2004). Nevertheless, although the simulated distributions of isopycnals from the two runs are relatively consistent, the $27.5\sigma_\theta$ isopycnal is slightly shallower in RUN2 than in RUN1. This is not consistent with

the fact that the penetration depth of anDIC is larger in RUN2 than in RUN1. This demonstrates that the main difference in anDIC penetration between the two runs, particularly in the equatorial region, is not due to interior isopycnal diffusion but due to advection or vertical diffusion.

The vertical distributions of salinity along 180°E are illustrated in Fig. 4, which clearly shows that the fresh water is transported from the high latitudes to the tropical Pacific, and forms the water mass named the North Pacific Intermediate Water (NPIW). The simulation is consistent with the observation (Fig. 4c), and the simulated salinity along the pathway of NPIW is smaller in RUN2 than in RUN1. This indicates that the transport of NPIW is strengthened in RUN2. The formation and transport of mode and intermediate waters is the primary mechanism for moving anDIC to intermediate depths (Sabine et al., 2004). As a result, more anDIC absorbed in the high latitudes is transported to the tropical Pacific by the NPIW. Based on this, the column inventory of anDIC in the tropical Pacific is increased in RUN2.

The zonal mean vertical distribution of anDIC in the Atlantic Ocean is shown in Fig. 5. Because of the transport of NADW, the penetration depth of anDIC in the North Atlantic Ocean is deeper than that in the North Pacific Ocean and the Southern Hemisphere. The data-based estimates show that the $5 \mu\text{mol kg}^{-1}$ contour can reach the deepest of 3500 m. Because of the influences of southward transport of NADW, the $5 \mu\text{mol kg}^{-1}$ contour can reach the 2000-m depth in the equatorial region. Our simulated results are basically in agreement with the data-based estimates. The deepest penetration of the $5 \mu\text{mol kg}^{-1}$ contour is about 3500 and 4000 m in RUN1 and RUN2, respectively. It can be seen from the difference in meridional stream-function between the two runs (RUN2–RUN1) that the deeper penetration of anDIC in the higher latitudes of North Atlantic in RUN2 is probably associated with the stronger NADW, which is due to the interannual change of the mixing processes in Northwest Atlantic. The largest strength of NADW obtained under the forcing of climatological data (RUN1) is 2 Sv smaller than that under the forcing of interannually

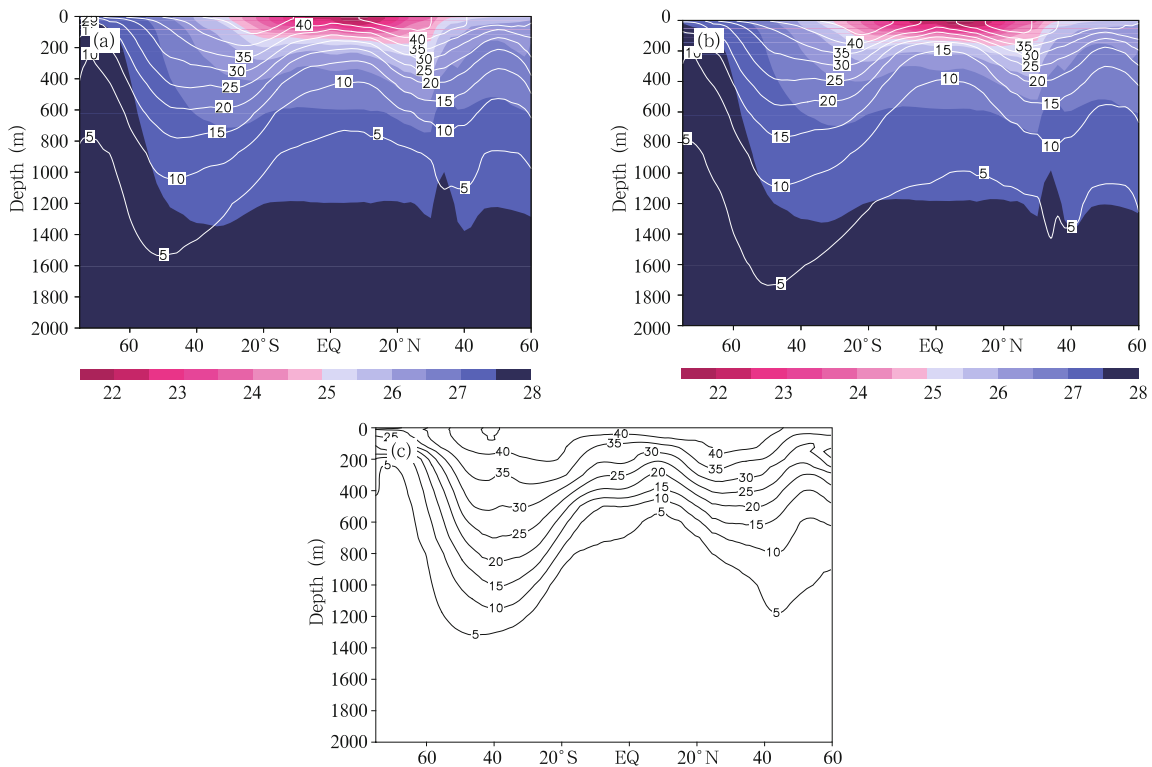


Fig. 3. Zonal mean vertical distributions of anthropogenic CO₂ ($\mu\text{mol kg}^{-1}$) in the Pacific and Indian Oceans. (a) RUN1, (b) RUN2, and (c) data-based results. Corresponding distributions of σ_θ are represented in color in (a) and (b).

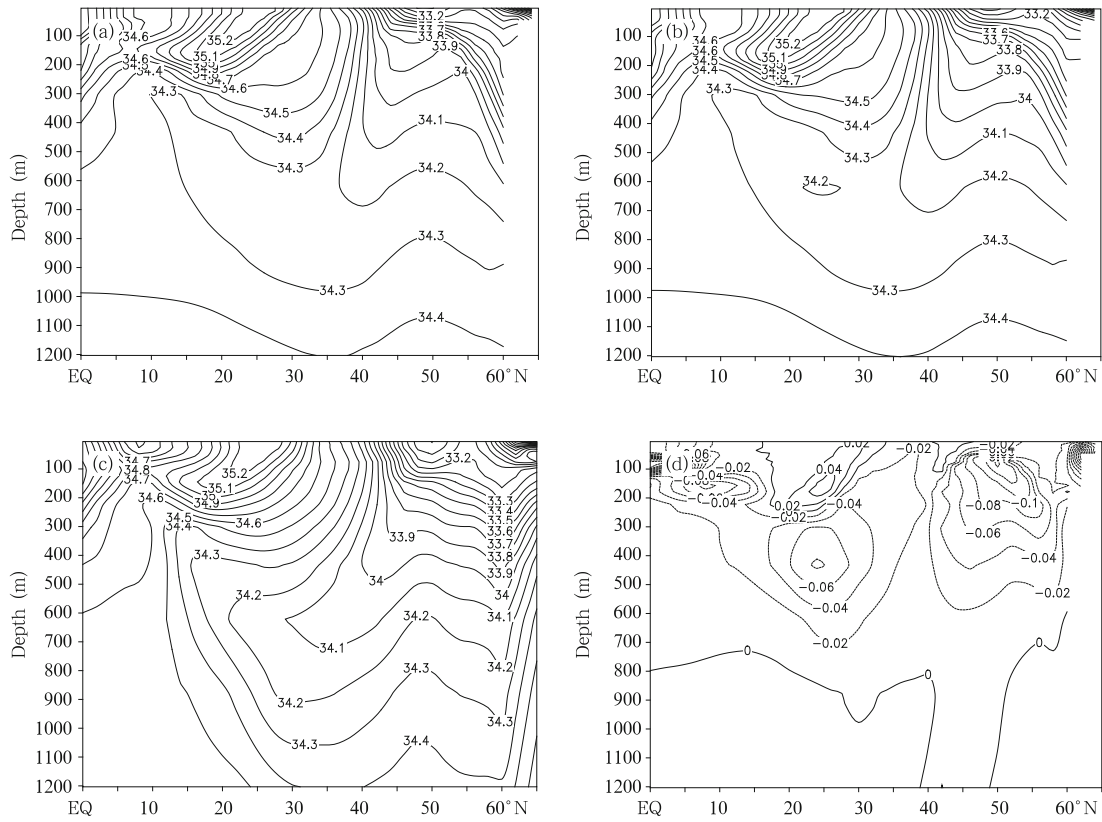


Fig. 4. Vertical distributions of salinity (g kg^{-1}) along 180°E . (a) RUN1, (b) RUN2, (c) WOA05, and (d) RUN2-RUN1.

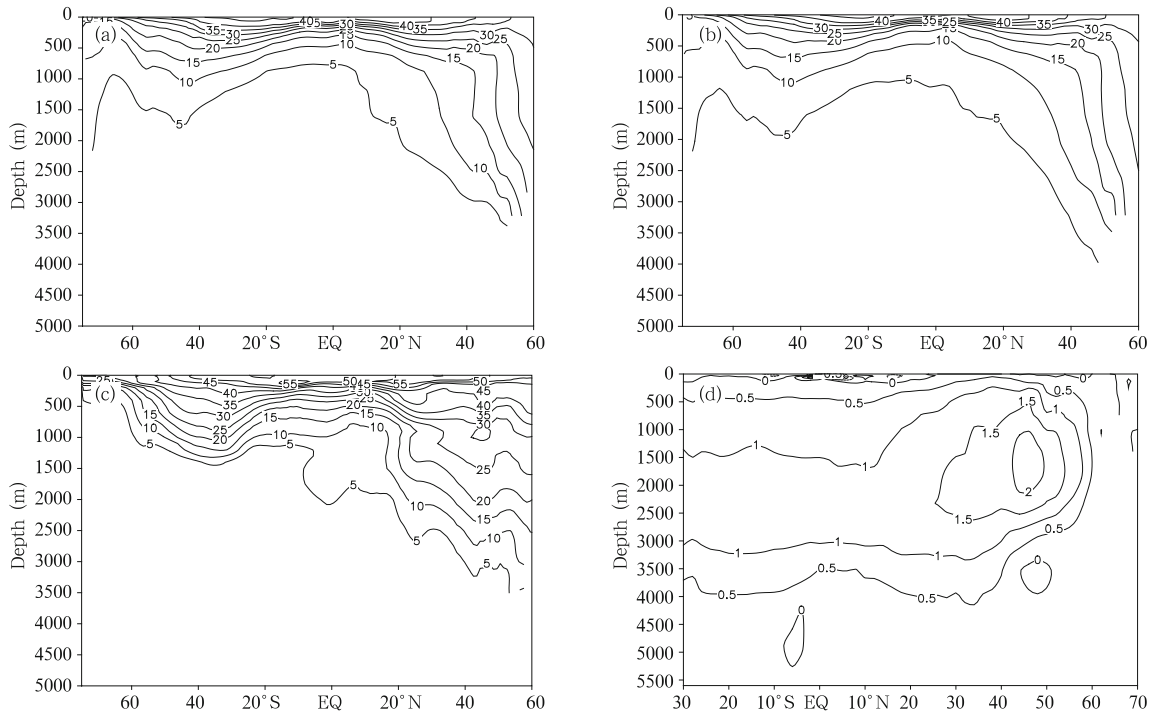


Fig. 5. Zonal mean vertical distributions of anthropogenic CO_2 ($\mu\text{mol kg}^{-1}$) in the Atlantic Ocean. (a) RUN1, (b) RUN2, (c) data-based results, and (d) difference of 50-yr averaged meridional stream function between the two runs (RUN2-RUN1) (in units of Sv, $1 \text{ Sv} = 10^6 \text{ m}^3 \text{ s}^{-1}$).

varying data. Therefore, in the lower latitudes of North Atlantic, the penetration of anDIC is obviously shallower in RUN1 than in RUN2. Near the equator, the penetration of the $5 \mu\text{mol kg}^{-1}$ contour in RUN1 is 200 m smaller than that in RUN2.

3.2 Uptake rates of anthropogenic CO_2

The difference in interior transport between the two runs affects the difference in surface anDIC concentrations (Fig. 1c), which can result in the difference in the air-sea anthropogenic carbon flux. Figure 6 shows the distribution of 10-yr averaged air-sea anthropogenic CO_2 flux in the 1990s. The main uptake areas are located in the equatorial Pacific Ocean, Northwest Pacific, Northwest Atlantic, and Southern Ocean. These areas all present strong vertical movement. These are the regions with large air-sea anthropogenic CO_2 fluxes and low surface anDIC concentrations. The main difference in the flux for the 1990s between the two runs is that in these main absorbing regions, the flux from RUN2 is slightly larger than that from RUN1, especially in the equatorial Pacific and the Southern Ocean.

It can be clearly seen from Fig. 7a that the air-sea anthropogenic carbon flux in RUN2 is larger than in RUN1. The results from the two runs indicate that the 1995 global air-sea anthropogenic carbon flux is $1.83 \text{ Pg C yr}^{-1}$ in RUN1 and $2.16 \text{ Pg C yr}^{-1}$ in RUN2, which are consistent with the data-based estimate and the inversion method result (Takahashi et al., 2002, Sweeny et al., 2007, Mikaloff Fletcher et al., 2006). The difference of the flux between the two runs increases with time. The slope of the regression line for the flux against time from RUN1 is $0.032 \text{ Pg C yr}^{-2}$, while the slope from RUN2 can reach $0.038 \text{ PgC yr}^{-2}$. Under the same forcing of atmospheric CO_2 and ice distributions, it can be seen from Eq. (1) that the difference in the flux between the two runs is probably caused by the differences in CO_2 solubility, wind speed at 10 m above sea level, and surface anDIC concentration. The CO_2 solubility is a function of surface temperature and salinity. Figure 7b shows the global area-averaged SST. It is known that before 1977, except for some individual years, the SST from RUN1 is generally higher than that from RUN2, while after 1977 the situation goes opposite. Under almost the

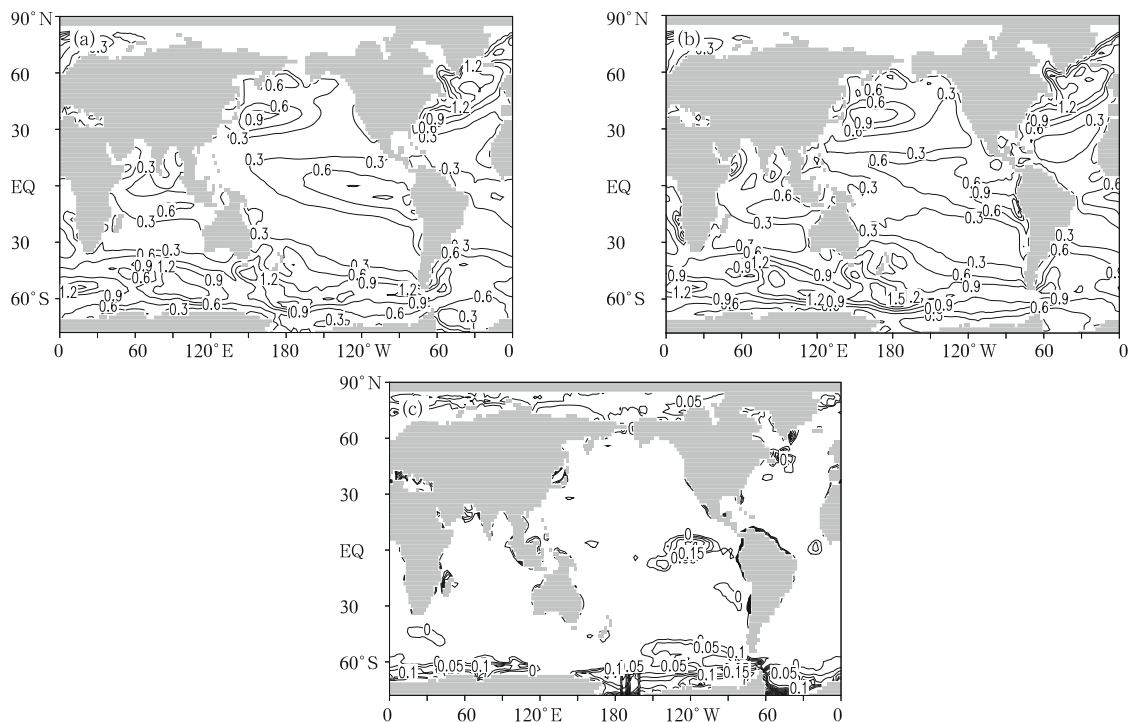


Fig. 6. Ten-year averaged distributions of air-sea anthropogenic carbon fluxes ($\text{mol m}^{-2} \text{ yr}^{-1}$) in the 1990s. (a) RUN1, (b) RUN2, and (c) RUN2-RUN1. Contour intervals are $0.3 \text{ mol m}^{-2} \text{ yr}^{-1}$ in (a, b) and $0.05 \text{ mol m}^{-2} \text{ yr}^{-1}$ in (c).

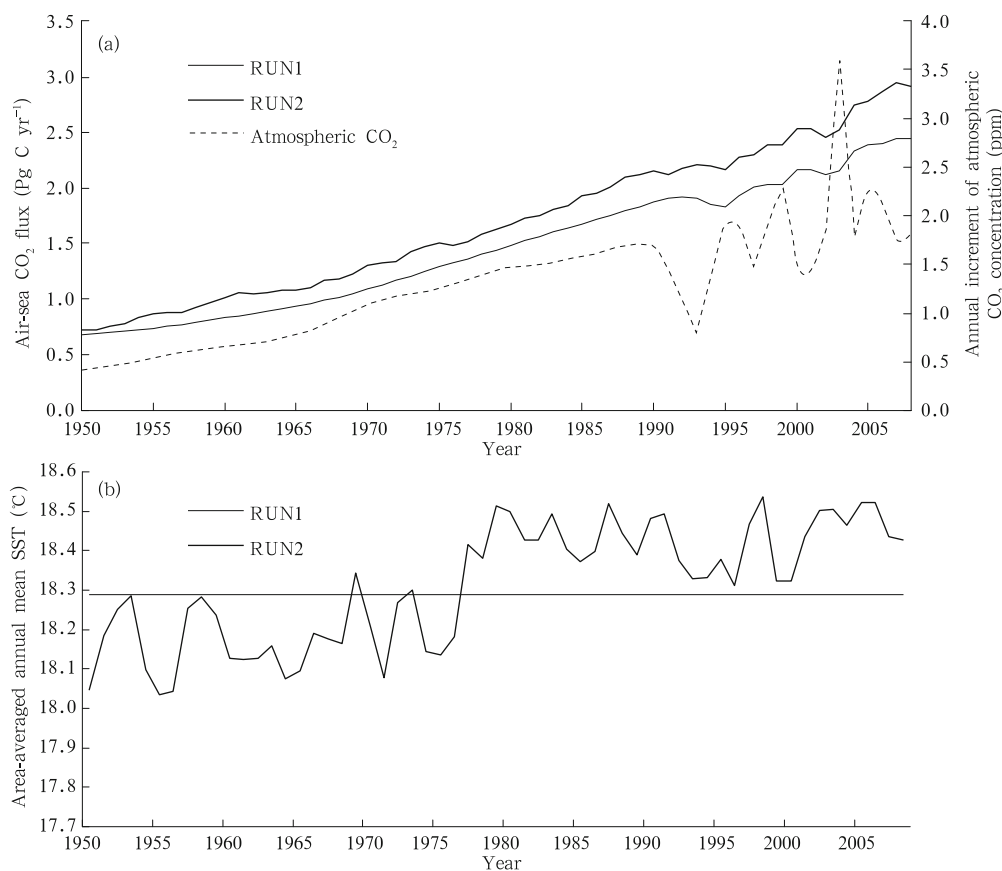


Fig. 7. Time series of (a) simulated air-sea exchange flux of anthropogenic CO₂ (Pg C yr⁻¹) and the annual increment of atmospheric CO₂ (ppm), and (b) area-averaged annual mean SST in RUN1 and RUN2.

same condition of salinity, SST becomes a sole factor for the difference of CO₂ solubility between the two runs. Hence, before 1977, the solubility from RUN1 was lower than that from RUN2. Small differences in surface anDIC occurred in the early period between the two runs, which is probably one of the reasons for the lower flux in RUN1. As time went on, particularly after 1977, with the lower solubility in RUN2, the flux from RUN2 was still higher than that from RUN1, which is probably related to the lower surface anDIC concentrations in RUN2. This demonstrates that the vertical transport rate of physical fields plays an important role in the adjustment of surface anDIC concentration and the uptake of anthropogenic CO₂.

The anthropogenic CO₂ fluxes from both runs increase with time, but with some fluctuations. This is related to strong interannual variations of atmospheric CO₂. As shown in Fig. 7a, the annual increment of atmospheric CO₂ concentrations reveals an obvi-

ous fluctuation in the 1990s. Under the equilibrium status of ocean physical fields, temporal variability of the annual increment of atmospheric CO₂ concentrations determines the variability of the flux. Thus, the anthropogenic CO₂ flux in RUN1 has an obvious fluctuation in the 1990s. On the basis of this fluctuation, the results from RUN2 are affected by the interannual variations of ocean physical fields; thus, in addition to the similar fluctuation to RUN1 in the 1990s, the flux in RUN2 also exhibits obvious fluctuations in other time periods. Compared with interannual variations of total carbon (anthropogenic carbon + natural carbon), which have been relatively much studied, the influence of interannual variations of physical fields on the anthropogenic carbon flux is relatively weak. In the main regions where there are strong interannual variations, such as the equatorial Pacific, the influences of interannual variations of physical fields on the natural carbon flux and on the anthropogenic carbon

flux are anti-phased. When vertical movement of water is constrained, the outgassing of natural carbon will be weakened, which means that both the natural carbon emissions and the anthropogenic carbon uptake will be restrained. Although the interannual variability of global carbon (natural + anthropogenic) fluxes from the model simulations, which is often represented by RMS (root mean square or σ), is different due to different models and different time periods in different studies, the RMS variability of global carbon fluxes obtained by different researchers from the monthly mean results is greater than or equal to $0.25 \text{ Pg C yr}^{-1}$. For example, McKinley et al. (2004) indicated that during the period 1980–1998, the RMS of global carbon fluxes is $0.28 \text{ Pg C yr}^{-1}$ (1σ). The result from Doney et al. (2009) shows that during the period 1979–2004, the RMS is $0.34 \text{ Pg C yr}^{-1}$ (1σ). Wetzel et al. (2005) analyzed the simulated results of 1979–2004, and gave a RMS of $0.50 \text{ Pg C yr}^{-1}$ (2σ). We compared our simulation results of anthropogenic carbon for the period 1950–2008 with that used in Wetzel et al. (2005). Using the monthly mean results, after removing the long-term trend and seasonal variations, we obtained the RMS of global anthropogenic carbon fluxes of about 0.1 Pg C yr^{-1} (1σ).

In order to examine the differences between re-

gions, we divide the global ocean into 10 regions (Fig. 8), in which the regional boundary is quite similar to that in Gruber et al. (2009). The numbers in Fig. 8 show the 1995 annual mean anthropogenic carbon flux and the RMS values (in parenthesis) for the period 1950–2008 from RUN2. Our results for the year 1995 are relatively consistent with those by Gruber et al. (2009) using the inversion method. The Southern Ocean has the largest uptake flux, and the tropical Pacific follows, while the subtropical South Atlantic has the smallest value. Specifically, the annual exchange flux reaches $1.01 \text{ Pg C yr}^{-1}$ in the Southern Ocean, which is much larger than the fluxes in other regions and also larger than the estimate of $0.75 \text{ Pg C yr}^{-1}$ by Gruber et al. (2009). The flux in the tropical Pacific is $0.40 \text{ Pg C yr}^{-1}$, which is larger than that in the tropical Indian Ocean and Atlantic. This is quite close to the estimate by Gruber et al. (2009). The region with large differences relative to the inversion method includes the subtropical Indian Ocean but excludes the Southern Ocean. The inversion method gives a flux of $0.24 \text{ Pg C yr}^{-1}$, which is much larger than our estimate of $0.12 \text{ Pg C yr}^{-1}$. The regions where there is a large difference in the anthropogenic carbon flux between our simulation and the inversion method are also the regions in which there is a large difference in

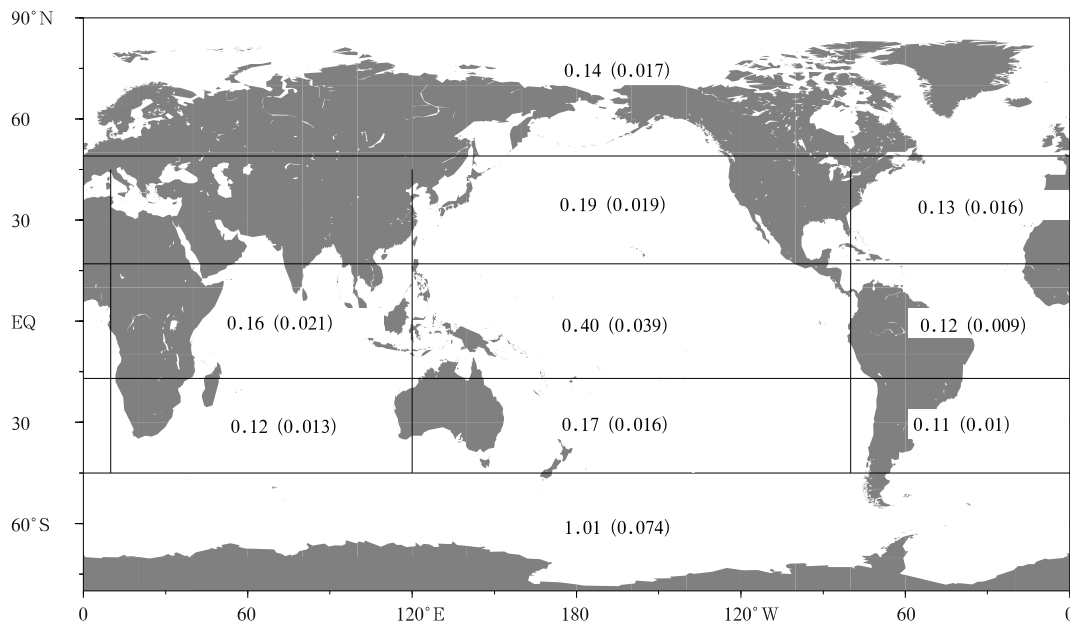


Fig. 8. Air-sea anthropogenic carbon fluxes (Pg C yr^{-1}) in different regions of the global ocean for the year 1995 and the RMS variability of the flux from 1950–2008 (numbers in parenthesis).

the total carbon flux between the inversion method and the $\Delta p\text{CO}_2$ -based method (Gruber et al., 2009). Therefore, the estimate of the anthropogenic carbon flux in the Southern Hemisphere needs to be further studied with more methods.

A comparison of regional results indicates that the variability of anthropogenic carbon fluxes in the Southern Ocean is the largest, with a RMS of $0.074 \text{ Pg C yr}^{-1}$. However, taking the area size, total fluxes, and other factors into consideration, the variability of anthropogenic carbon fluxes in the tropical Pacific becomes more significant. This is associated with the strongest annual fluctuation signals of physical fields in the tropical Pacific. According to the simulated results, Le Quéré et al. (2000) pointed out that because of the ENSO events, interannual variability of tropical Pacific air-sea carbon fluxes accounts for 70% of the interannual variability of global air-sea carbon fluxes. McKinley et al. (2004) obtained a RMS of $0.17 \text{ Pg C yr}^{-1}$ for the tropical Pacific (15°S – 15°N) air-sea carbon flux. Thus, it can be inferred that the RMS variability in the anthropogenic carbon flux is obviously smaller than that in the total carbon flux. Furthermore, because of the impact of the large anthropogenic carbon flux in the western North Pacific and western North Atlantic, the RMS variability of the anthropogenic carbon flux in the northern subtropical region is slightly larger than that in the same latitudinal bands of the Southern Hemisphere.

4. Conclusions

A global ocean general circulation model LICOM with a horizontal resolution of $2^\circ \times 2^\circ$ has been employed to estimate the influence of the climate change on the uptake and storage of anthropogenic CO_2 in the global ocean. The perturbation method for the calculation of air-sea anthropogenic CO_2 fluxes by Sarmiento et al. (1992) was adopted. Two numerical experiments were conducted: the control run (RUN1) with the climatological daily mean forcing data and the climate change run (RUN2) with the interannually varying daily mean forcing data from NCEP. The simulated distributions of anthropogenic carbon from both runs are consistent with the data-based esti-

mates, indicating that the perturbation method is appropriate for the estimation of anthropogenic carbon.

A comparison of the two simulations shows that with the interannual variations of the forcing, the transport of the main water masses is enhanced because of the interannual change of the mixing processes. The physical ventilation rate is larger in RUN2 than in RUN1; the largest strength of NADW in RUN2 is 2 Sv larger than in RUN1. This is also confirmed by the difference in the interior transport of anthropogenic carbon between the two runs. Although the air-sea anthropogenic carbon flux from RUN2 is larger than that from RUN1, anthropogenic carbon concentrations in the upper ocean in RUN2 are smaller than those in RUN1 and are closer to the data-based estimates. The difference in the large-scale circulation results in the obviously deeper penetration of anthropogenic carbon in RUN2 than in RUN1. Even below the 1000-m depth, penetration of the simulated $5 \mu\text{mol kg}^{-1}$ contour is deeper than the data-based estimate, which leads to the larger anthropogenic carbon inventory in most regions in RUN2 than in RUN1.

The low surface anDIC concentration in RUN2 enhances the oceanic uptake of anthropogenic carbon. From 1950 to 2008, the air-sea anthropogenic carbon flux was higher in RUN2 than in RUN1, even during the 1990s when the SST was higher in RUN2 than in RUN1. Our simulations show that the global oceanic uptake of anthropogenic carbon was 1.83 and 2.16 Pg C yr^{-1} in RUN1 and RUN2 for 1995, respectively, which are within the range of the estimates using the data and the inversion method. Meanwhile, our simulation results indicate that as of 1994, the global ocean contained 99 and 107 Pg C of anthropogenic carbon in RUN1 and RUN2, respectively, which are also within the range of the data-based estimates.

In the 10 regions of the global ocean, both annual uptake of anthropogenic carbon and its RMS variability in the regions south of 45°S are much larger than those in other regions. When the area size, flux magnitude, and other factors are taken into account, the RMS variability of the air-sea anthropogenic carbon flux in the tropical Pacific is more significant. According to the simulated monthly mean results, the RMS variability of global air-sea anthropogenic carbon flux

is 0.1 Pg C yr^{-1} during 1950–2008, about one third of the RMS variability of the global total carbon flux. However, the anthropogenic carbon flux and total carbon flux are not in phase. The relationship between the two needs a further examination.

REFERENCES

- Bacastow, R., and E. Maier-Reimer, 1990: Ocean-circulation model of the carbon cycle. *Climatic Dyn.*, **4**, 95–125.
- Bender, M., D. T. Ho, M. B. Hendricks, et al., 2005: Atmospheric O_2/N_2 changes, 1993–2002: Implications for the partitioning of fossil fuel CO_2 sequestration. *Global Biogeochem. Cycles*, **19**, GB4017, doi: 10.1029/2004GB002410.
- Danabasoglu, G., and J. C. McWilliams, 1995: Sensitivity of the global ocean circulation to parameterizations of mesoscale tracer transports. *J. Climate*, **8**, 2967–2987.
- Doney, S. C., K. Lindsay, K. Caldeira, et al., 2004: Evaluating global ocean carbon models: The importance of realistic physics. *Global Biogeochem. Cycles*, **18**, doi: 10.1029/2003GB002510.
- , I. Lima, R. A. Feely, et al., 2009: Mechanisms governing interannual variability in upper-ocean inorganic carbon system and air-sea CO_2 fluxes: Physical climate and atmospheric dust. *Deep-Sea Res. II*, **56**, 640–655.
- Dong Tiaoling, Wang Mingxing, and Liu Ruizhi, 1994: Two-dimensional atmospheric CO_2 -Atlantic carbon cycle model. *Chinese J. Atmos. Sci.*, **18**, 631–640. (in Chinese)
- Duffy, P. B., K. Caldeira, J. Selvaggi, et al., 1997: Effects of subgrid-scale mixing parameterizations on simulated distributions of natural ^{14}C , temperature, and salinity in a three-dimensional ocean general circulation model. *J. Phys. Oceanogr.*, **27**, 498–523.
- England, M. H., and A. C. Hirst, 1997: Chlorofluorocarbon uptake in a World Ocean model 2. Sensitivity to surface thermohaline forcing and subsurface mixing parameterizations. *J. Geophys. Res.*, **102**, 15709–15731.
- Enting, I. G., T. M. L. Wigley, and M. Heimann, 1994: Future Emissions and Concentration of Carbon Dioxide: Key Ocean/Atmosphere/Land Analysis. CSIRO Division of Atmospheric Research Technical Paper No. 31, CSIRO, Australia, 133 pp.
- Gent, P. R., and J. C. McWilliams, 1990: Isopycnal mixing in ocean circulation models. *J. Phys. Oceanogr.*, **20**, 150–155.
- , —, T. J. McDougall, et al., 1995: Parameterizing eddy-induced tracer transports in ocean circulation models. *J. Phys. Oceanogr.*, **25**, 463–474.
- Gloor, M., N. Gruber, J. L. Sarmiento, et al., 2003: A first estimate of present and pre-industrial air-sea CO_2 fluxes patterns based on ocean interior carbon measurements and models. *Geophys. Res. Lett.*, **30**(1), 1010, doi: 10.1029/2002GL015594.
- Gruber, N., J. L. Sarmiento, and T. F. Stocker, 1996: An improved method for detecting anthropogenic CO_2 in the oceans. *Global Biogeochem. Cycles*, **10**(4), 809–837, doi: 10.1029/96GB01,608.
- , and C. D. Keeling, 2001: An improved estimate of the isotopic air-sea disequilibrium of CO_2 : Implications for the oceanic uptake of anthropogenic CO_2 . *Geophys. Res. Lett.*, **28**(3), 555–558, doi: 10.1029/2000GL011853.
- , M. Gloor, S. E. Mikaloff Fletcher, et al., 2009: Oceanic sources, sinks, and transport of atmospheric CO_2 . *Global Biogeochem. Cycles*, **23**, GB1005, doi: 10.1029/2008GB003349.
- Gurney, K. R., et al., 2004: Transcom 3 inversion inter-comparison: Model mean results for the estimation of seasonal carbon sources and sinks. *Global Biogeochem. Cycles*, **18**, GB1010, doi: 10.1029/2003GB002111.
- Jin Xin and Shi Guangyu, 2001: The role of biological pump in ocean carbon cycle. *Chinese J. Atmos. Sci.*, **25**, 683–688. (in Chinese)
- Joos, F., R. Meyer, M. Bruno, et al., 1999: The variability in the carbon sinks as reconstructed for the last 1000 years. *Geophys. Res. Lett.*, **26**, 1437–1441.
- Key, R. M., A. Kozyr, C. L. Sabine, et al., 2004: A global ocean carbon climatology: Results from Global Data Analysis Project (GLODAP). *Global Biogeochem. Cycles*, **18**, doi: 10.1029/2004GB002247.
- Khatiwala, F. Primeau, and T. Hall, 2009: Reconstruction of the history of anthropogenic CO_2 concentrations in the ocean. *Nature*, **462**, doi: 10.1038/nature08526.
- Le Quééré, C., J. C. Orr, P. Monfray, et al., 2000: Interannual variability of the oceanic sink of CO_2 from 1979 through 1997. *Global Biogeochem. Cycles*, **14**(4), 1247–1265.
- Levine, N. M., S. C. Doney, R. Wanninkhof, et al., 2008: Impact of ocean carbon system variability on the detection of temporal increases in anthropogenic CO_2 . *J. Geophys. Res.*, **113**, doi: 10.1029/2007JC004153.

- Levitus, S., and T. P. Boyer, 1994: *World Ocean Atlas 1994 Volume 4: Temperature*. NOAA Atlas NESDIS 4, NODC, Washington D. C., 117 pp.
- , R. Burgett, and T. P. Boyer, 1994: *World Ocean Atlas 1994 Volume 3: Salinity*. NOAA Atlas NESDIS 3, NODC, Washington D. C., 99 pp.
- Liu, H. L., X. H. Zhang, W. Li, et al., 2004: An eddy-permitting oceanic general circulation model and its preliminary evaluation. *Adv. Atmos. Sci.*, **21**, 675–690.
- Maier-Reimer, E., and K. Hasselmann, 1987: Transport and storage of CO₂ in the ocean—an inorganic ocean-circulation carbon cycle model. *Climatic Dyn.*, **2**, 63–90.
- Manning, A. C., and R. F. Keeling, 2006: Global oceanic and land biotic carbon sinks from the Scripps atmospheric oxygen flask sampling network. *Tellus B*, **58**, 95–116.
- McKinley, G. A., M. J. Follows, and J. Marshall, 2004: Mechanisms of air-sea CO₂ flux variability in the equatorial Pacific and the North Atlantic. *Global Biogeochem. Cycles*, **18**, GB2011, doi: 10.1029/2003GB002179.
- McWilliams, J. C., and Coauthors, 1983: The local dynamics of eddies in the western North Atlantic. *Eddies in Marine Science*. A. R. Robinson, Ed., Springer-Verlag, 92–113.
- Mikaloff Fletcher, S. E., N. Gruber, A. R. Jacobson, et al., 2006: Inverse estimates of anthropogenic CO₂ uptake, transport, and storage by the ocean. *Global Biogeochem. Cycles*, **20**, GB2002, doi: 10.1029/2005GB002530.
- Obata, A., and Y. Kitamura, 2003: Interannual variability of sea-air exchange of CO₂ from 1961 to 1998 with a global ocean circulation biogeochemistry model. *J. Geophys. Res.*, **108** (C11), doi: 10.1029/2001JC001088.
- Orr, J. E. Maier-Reimer, U. Mikolajewicz, et al., 2001: Estimates of anthropogenic carbon uptake from four 3-D global ocean models. *Global Biogeochem. Cycles*, **15**, 43–60.
- Pu Yifen and Wang Mingxing, 2001: An ocean carbon cycle model. Part II: Simulation analysis on the Indian Ocean. *Climatic Environ. Res.*, **6**, 67–76. (in Chinese)
- Rodgers, K. B., O. Aumont, C. Menkes, et al., 2008: Decadal variations in equatorial Pacific ecosystems and ferrocline/pycnocline decoupling. *Global Biogeochem. Cycles*, **19**, GB2019, doi: 10.1029/2006GB002919.
- Sabine, C. L., R. A. Feely, N. Gruber, et al., 2004: The oceanic sink for anthropogenic CO₂. *Science*, 367–371.
- Sarmiento, J. L., J. C. Orr, and U. Siegenthaler, 1992: A perturbation simulation of CO₂ uptake in an ocean general circulation model. *J. Geophys. Res.*, **97**, 3621–3645.
- Six, K. D., and E. Maier-Reimer, 1996: Effects of plankton dynamics on seasonal carbon fluxes in an ocean general circulation model. *Global Biogeochem. Cycles*, **10**(4), 559–583.
- Solomon, S., D. H. Qin, M. Manning, et al., 2007: *Climate Change 2007: The Physical Science Basis*. Cambridge University Press, Cambridge, United Kingdom and New York, NY, USA, 996 pp.
- Sundquist, E. T., 1993: The global carbon dioxide budget. *Science*, **259**, 934–941.
- Sweeney, C., E. Gloor, A. R. Jacobson, et al., 2007: Constraining global air-sea gas exchange for CO₂ with recent bomb ¹⁴C measurements. *Global Biogeochem. Cycles*, **21**, GB2015, doi: 10.1029/2006GB002784.
- Takahashi, T., S. C. Sutherland, C. Sweeney, et al., 2002: Global sea-air CO₂ flux based on climatological surface ocean pCO₂, and seasonal biological and temperature effects. *Deep-Sea Res. II*, **49**, 1601–1622.
- Wang, X., J. R. Christian, R. Murtugudde, et al., 2006: Spatial and temporal variability of the surface water pCO₂ and air-sea CO₂ flux in the equatorial Pacific during 1980–2003: A basin-scale cycle model. *J. Geophys. Res.*, **111**, C07S04, doi: 10.1029/2005JC002972.
- Wanninkhof, R., 1992: Relationship between wind speed and gas exchange over the ocean. *J. Geophys. Res.*, **9**, 7373–7382.
- Waugh, D. W., T. M. Hall, B. I. McNeil, et al., 2006: Anthropogenic CO₂ in the oceans estimated using transit time distributions. *Tellus B*, **58**(5), 376–389.
- Wetzel, P., A. Winguth, and E. Maier-Reimer, 2005: Sea-to-air CO₂ flux from 1948 to 2003: A model study. *Global Biogeochem. Cycles*, **19**, GB2005, doi: 10.1029/2004GB002339.
- Xing Runan, 2000: A three-dimensional world ocean carbon cycle model with ocean biota. *Chinese J. Atmos. Sci.*, **24**, 333–340. (in Chinese)
- Xu, Y. F., and Y. C. Li, 2009: Estimates of anthropogenic CO₂ uptake in a global ocean model. *Adv. Atmos. Sci.*, **26**(2), 265–274, doi: 10.1007/s00376-0265-z.